RESEARCH ARTICLE | MARCH 17 2020

Revealing nanoscale dynamics during an epoxy curing reaction with x-ray photon correlation spectroscopy FREE

Special Collection: Polymer-Grafted Nanoparticles

Benjamin M. Yavitt [ORCID] ; Daniel Salatto; Zhixing Huang; Yuto T. Koga; Maya K. Endoh; Lutz Wiegart;
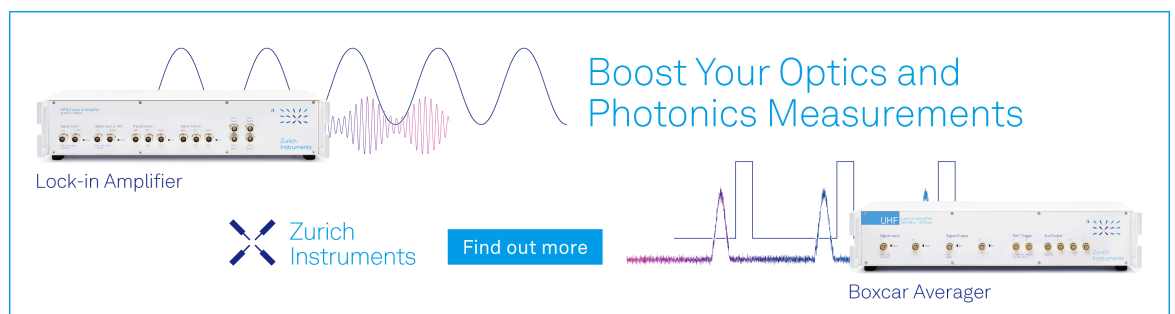Sascha Poeller [ORCID] ; Stanislas Petrash [✉] ; Tadanori Koga [✉] [ORCID]

Check for updates

CHORUS

View Online   Export Citation

Revealing nanoscale dynamics during an epoxy curing reaction with x-ray photon correlation spectroscopy

View Online   Export Citation   CrossMark

Benjamin M. Yavitt,[1,2] (iD) Daniel Salatto,[1] Zhixing Huang,[1] Yuto T. Koga,[3] Maya K. Endoh,[1] Lutz Wiegart,[2]
Sascha Poeller,[4] (iD) Stanislas Petrash,[5,a] and Tadanori Koga[1,a] (iD)

AFFILIATIONS

[1] Department of Materials Science and Chemical Engineering, Stony Brook University, Stony Brook, New York 11794-2275, USA
[2] National Synchrotron Light Source II, Brookhaven National Laboratory, Upton, New York 11973, USA
[3] Department of Food Science, College of Agriculture and Life Sciences, Cornell University, Ithaca, New York, 14853, USA
[4] Adhesive Technologies, Henkel AG & Co KGaA, 40589 Duesseldorf, Germany
[5] Adhesive Technologies, Henkel Corporation, Bridgewater, New Jersey 08807, USA

Note: This paper is part of the Special Topic on Polymer-Grafted Nanoparticles.
[a]**Authors to whom correspondence should be addressed:** stan.petrash@henkel.com and tadanori.koga@stonybrook.edu

ABSTRACT

The evolution of nanoscale properties is measured during the thermally triggered curing of an industrial epoxy adhesive. We use x-ray photon correlation spectroscopy (XPCS) to track the progression of the curing reaction through the local dynamics of filler particles that reflect the formation of a thermoset network. Out-of-equilibrium dynamics are resolved through identification and analysis of the intensity–intensity autocorrelation functions obtained from XPCS. The characteristic time scale and local velocity of the filler is calculated as functions of time and temperature. We find that the dynamics speed up when approaching the curing temperature (T_{cure}), and decay rapidly once T_{cure} is reached. We compare the results from XPCS to conventional macroscale characterization by differential scanning calorimetry (DSC). The demonstration and implementation of nanoscale characterization of curing reactions by XPCS proves useful for future development and optimization of epoxy thermoset materials and other industrial adhesive systems.

INTRODUCTION

Epoxy thermosets are ubiquitous materials with many applications in a wide range of industries. Epoxies are used as adhesives, coatings, and structural materials.[1] Their versatility is beneficial for an array of arenas such as aerospace, construction, or automotive applications. These materials are also found in more demanding applications such as microelectronics or personal/home care. Epoxies are tough materials that possess good thermomechanical properties, are chemically resistant, and exhibit strong adhesion to a variety of substrates.[1,2] Industrially relevant epoxy resins often contain active fillers (such as inorganic nanoparticles) to improve material properties or to control the curing reaction.[3] Therefore, epoxy adhesives are an important class of polymeric nanocomposites.

Epoxy adhesives owe their mechanical and chemical stability to the controlled formation of a three-dimensional cross-linked thermoset network. The network is generally formed from a monomeric or prepolymeric resin that "cures" after the introduction of an external trigger.[4] Epoxies are defined by the oxirane moiety: two carbons and an oxygen bonded together in a three-membered ring.[5] Ring opening of oxiranes can proceed via an electrophilic reaction pathway, which is a cationic homo-polymerization of the epoxy resin.[1,6,7] The epoxy ring is activated by a strong electrophile (e.g., Lewis acids) and reacts with a hydroxy group to form a polyether thermoset. Epoxy resins also react via a nucleophilic homo-polymerization with a nucleophilic initiator (e.g., imidazoles) to form a polyether thermoset, or alternatively through nucleophilic

04 April 2024 17:16:59

polyaddition reactions with hardeners containing an active hydrogen (e.g., primary and secondary amines, thiols, carboxylic acids, acid anhydrides, phenols).[8] Depending on the type of hardener, the nucleophilic polyaddition of epoxies may occur directly without the need of further initiators.[8–12] Other hardeners require initiation reactions to generate the reactive nucleophile (thiols, acid anhydrides), which undergoes a ring opening reaction with the oxirane ring. Various polymers are obtained by the polyaddition reaction of epoxy resins and hardener, e.g., polyether (phenols), polyetheramine, polyether-polythioether or polyester (carboxylic acids, acid anhydrides).[4]

Typically, the curing reaction is initiated by mixing two reactive components together (A + B) or by using temperature or ultra-violet (UV) light to initiate the cross-linking through a catalyst or reactive group.[1] While the chemistry of epoxidation is generally well understood, there is still considerable effort to improve and engineer the structure and mechanical properties of epoxies for an ever-increasing range of desired applications.[5] Thus, our understanding of structure–property relationship in epoxy thermosets must be continually updated.

As previously mentioned, the cross-linking reaction is at the heart of the material properties. As prepolymer resin reacts, the irreversible thermoset network forms that defines the final properties of the cured material. Controlling the curing pathways and kinetics is of upmost importance. A detailed understanding of the progress of the cure reaction is especially relevant for bonding of different substrates with heat curing adhesives (e.g., glass to metal/ metal to plastic bonding), since the development of the cross-linked network with time determines the mechanical stress in the adhesive bond line created due to the substrate mismatch. The progress of the cure reaction is especially important in asymmetric heat curing processes. The time-resolved development of modulus, glass transition temperature (T_g), and extent of cross-linking are crucial factors that determine structural heterogeneities in the bonded part induced by the temperature gradient and heating rate.[13]

The kinetics of curing are typically measured by macroscale characterization techniques such as rheology or differential scanning calorimetry (DSC).[14–16] In rheology, a liquid to solid transition is identified as the zero-shear viscosity diverges and a gel structure is formed.[17,18] The cross-linking continues to progress beyond the gel point as the dynamic moduli increase significantly. The traditional mechanical methods to characterize the curing behavior of heat curing epoxy resins are limited when resolving the later stages of the cross-linking reaction, and thus fail to provide a full picture of the cross-linking progress. In thermal characterization techniques such as DSC, an exothermic event is observed as the cross-linking initiates and progresses.[16] For thermally triggered materials, the cross-linking can be tracked through isothermal measurements or temperature ramps through the curing temperature (T_{cure}).[16] The macroscale engineering material properties (modulus, adhesion, and chemical resistance) are derived from the structure formation on the microscale and nanoscale. Therefore, the direct measurement of microscopic behavior during curing is of particular interest, specifically targeted to the length scale of the macromolecular network (or correlation length on the order of 1–100 nm) or the chemical moieties themselves. Significant work showed that spectroscopy such as *in situ* near-IR (NIR) absorption spectroscopy or Raman spectroscopy can

monitor the reaction kinetics.[15,16,19–22] For example, recent reports tracked the curing of a model thermosetting epoxy resin through the NIR signature of aromatic rings in the prepolymer backbone which were considered as molecular probes. The NIR absorbance shifted as the reaction of monomers in the prepolymer resin progressed and the results are correlated to characterization by DSC.[15]

In addition to the relevant length scales, the time scale of macromolecular motion (the polymer dynamics) is important for properties such as viscous flow, curing speed, and toughness.[23,24] A variety of fillers, most often inorganic micro- and nano-powders with engineered properties are commonly used to control the processing and achieve desired properties of the polymer/filler nanocomposite.[25] The development of stronger dynamics–property relationships is necessary to carefully tune the material during cross-linking. X-ray photon correlation spectroscopy (XPCS) is a powerful tool to resolve dynamics on the nanoscale in polymeric materials. XPCS is a scattering technique that utilizes partially coherent X-rays to obtain time-resolved information about the dynamics of scatterers in a complex fluid.[23] The interaction of a coherent x-ray beam with electron density fluctuations (such as inorganic nanoparticles in a polymer matrix) produces a "speckle pattern" on a two-dimensional (2D) area detector. From a time series of speckle patterns, the dynamics of the scatterers are quantified via intensity–intensity autocorrelation functions. Typical synchrotron based XPCS is able to resolve dynamics over a wide range of time scales (from sub millisecond up to tens of thousands of seconds) over relevant length scales (nm to μm) in polymer nanocomposites.[26] Advancements in technique development and detector technology are extending the time scales to even faster dynamics.[27,28] In addition to probing dynamics, XPCS also provides unique information with a spatial resolution in the micrometer range, corresponding to the focal spot size of the x-ray beam. Here, we use XPCS to monitor the evolution of dynamics and structure during the thermal cross-linking of an industrial epoxy. While dynamic light scattering (DLS) and XPCS have been used to characterize cross-linking in many model systems, no such technique has been used to understand epoxy curing in industrial materials.[29–33] XPCS is well-suited to resolve quantitative dynamic behavior unobtainable by other techniques and complements conventional DSC measurements. While the epoxy curing chemistry is well known and studied, XPCS provides a new viewpoint to quantitatively describe the curing process.

EXPERIMENTAL

A model industrial epoxy adhesive was formulated and supplied by Henkel Corp. We used a cationically, homo-polymerized one-component heat curable LOCTITE® 3536 CSP epoxy resin with a cationic catalyst. The formulation contained 25 wt. % alumina trihydrate filler (diameter ~2 μm) and a smaller fraction of 1.5 wt. % boron nitride platelets for thermal stability and viscosity modification. Scanning electron microscopy (SEM) images of fillers are shown in Fig. S1 of the supplementary material. In addition to providing mechanical and thermal stability to the epoxy resin, the alumina filler acts as a marker to resolve the dynamics of epoxy during a curing process.[24,34] Note that boron nitride platelets also give rise to the scattering. However, the small beam size, which is about five times smaller than the large platelets (~80 μm according

04 April 2024 17:16:59

to the SEM image), and coherence limitation do not allow measurement of such large particles. In fact, as will be discussed later, we can see power-law scattering with an exponent of approximately -4 in the scattering profile from the sample, indicating that the contributions from the platelets, which should give rise to power-law scattering with an exponent of -2, are minimal within the observed q range. The particles are an industrial formulation with large dispersity, which was estimated by SEM. The recommended curing schedule for the resin is as follows: heat to $T = 85\,°C$ and equilibrate for 10 min, increase temperature to the curing temperature $T_{cure} = 120\,°C$, followed by isothermal treatment at T_{cure} for 20 min.

The sample was used as received with no further modification. For scattering measurements, the bulk epoxy paste was filled into a circular sample holder backed with $25\,\mu m$ thick polyamide (PIT1 N, Caplinq) windows and sealed. The sample thickness was fixed to 0.5 mm. XPCS was performed on Beamline 11-ID, CHX (Coherent Hard X-Ray Scattering) at National Synchrotron Light Source II, Brookhaven National Laboratory, Upton, NY, USA. A partially coherent x-ray beam with energy of 9.65 keV (wavelength $\lambda = 0.128\,nm$) and an unattenuated flux of 3×10^{11} ph/s was focused into a spot size with a $10\,\mu m$ diameter at the sample in a transmission geometry. Speckle patterns were collected on an Eiger X 4 M (Dectris) pixelated photon counting detector at a sample-to-detector distance of 16 m. The holder was placed into a temperature-controlled cryo-furnace equipped with Pt100 temperature sensors for temperature measurement and control. The chamber was preheated to $T = 85\,°C$ and allowed to equilibrate for 10 min. After adequate temperature stability, several series of XPCS datasets were collected with predetermined frame rates, frame numbers, total exposure times, and attenuations. The frame rates and frame numbers were tailored to capture dynamics at fast (0.05–10 s) and slow (100–1000 s) time scales, respectively. Radiation damage was evaluated and mitigated by attenuation of the beam with double-sided polished silicon wafers and a millisecond fast shutter.[35] Figure S2 shows dynamics overlap between each data set collected in the isothermal precure state ($T = 85\,°C$) and cured stage ($T = 120\,°C$), suggesting the total dose exposure (TDE) is below the threshold for radiation damage. Sample translations by several x-ray beam sizes were used in between each dataset to avoid accumulation of x-ray dose in a single spot. The sample was then heated according to the previously described curing schedule at a rate of 5 °C/min to $T = 120\,°C$ while the continuous series of XPCS scans were performed, measuring the in situ dynamics. All analyses of scattering data and calculations of autocorrelation functions were performed using CHX beamline Python code and computing infrastructure (NSLS-II GitHub).[36]

Differential scanning calorimetry (DSC) was performed on a PerkinElmer Pyris Diamond DSC. Approximately 15 mg of epoxy paste was placed in a hermetically sealed aluminum sample pan. The sample pan was placed in the DSC at an equilibrated temperature of $T = 50\,°C$. The sample chamber was then heated to $T = 85\,°C$ and equilibrated for 10 min. The temperature was increased to $T = 120\,°C$ at a ramp rate of 5 °C/min. Once $T = 120\,°C$ was reached, the temperature was stabilized for up to 30 min. Following the curing schedule, the sample was returned to a stabilized temperature of $T = 50\,°C$. A second, identical temperature scan was performed on the same sample, simulating the response of a cured epoxy. The normalized heat flow (in W/g) was recorded as a function of time and plotted alongside the sample temperature.

Scanning Electron Microscopy of filler particles was performed on a FEI Verios 460 XHR SEM at a 5 keV accelerating voltage. The specimen was not sputter-coated with conductive coating to best preserve particle surface morphology.

RESULTS AND DISCUSSION

The curing schedule of the epoxy sample is predefined according to the supplier (Henkel). Therefore, we expect the prepolymer resin to cross-link into a thermosetting network, triggered by the thermally activated catalyst. The nanoscale motion of the alumina trihydrate fillers is measured by XPCS during the activation and the onset of the curing reaction. We hypothesize that the motion of the particles is directly related to the evolution of the polymer network structure surrounding the particles. Therefore, we expect the particle motion to probe the extent of the curing reaction through their evolving dynamics.[34,37,38]

In XPCS, dynamics are resolved through an intensity–intensity auto correlation function g_2 [Eq. (1)], which is derived from the time series of speckle patterns collected on the 2D area detector during the XPCS measurements,

$$g_2(q, \tau) = \frac{\langle I(q, t)I(q, t + \tau)\rangle}{\langle I(q, t)\rangle^2},$$ (1)

where q is the wavevector $q = 4\pi\sin(\theta)/\lambda$ with 2θ being the scattering angle in a small angle geometry and τ is the delay time. The average $\langle\cdots\rangle$ is performed over all detector pixels corresponding to the same magnitude of the wavevector as well as over time. The g_2 functions reveal the characteristic relaxation time of the observed dynamics within the cross-linking epoxy material. The correlation functions are q dependent, and, therefore, resolve motion across a wide span of length scales dependent on the scattering geometry. In the small angle scattering geometry used in this study, the nanoscale motion is resolved over length scales of order 10–100 nm, more relevant for the mesh size in a cross-linking polymeric system. In the case of a cross-linking reaction, we expect the system to be "out-of-equilibrium." In other words, if the cross-linking reaction is rapid, the structure and corresponding dynamics are likely changing on the time scale of the experiment. The one-time correlation function in Eq. (1), describing equilibrium dynamics, will not correctly describe such a phenomenon. Therefore, a two-time correlation function is necessary [Eq. (2)], which defines the intensity–intensity autocorrelation for any respective times t_1 and t_2 in the time series where the average $\langle\cdots\rangle$ is performed over all detector pixels corresponding to the same magnitude of the wavevector but not over time,[39,40]

$$C(q, t_1, t_2) = \frac{\langle I(q, t_1)I(q, t_2)\rangle}{\langle I(q, t_1)\rangle\langle I(q, t_2)\rangle}.$$ (2)

The two-time correlation is typically represented as a 2D plot along separate axis of the respective times t_1 and t_2.[39] Due to the

04 April 2024 17:16:59

"out-of-equilibrium" nature of the reaction, the two-time correlation plots must be quantitatively evaluated at various "average" times during the time series. We define such a time as an average "aging" time $t_{age} = (t_1 + t_2)/2$.[41] Schematically, t_{age} progresses along the diagonal ($t_1 = t_2$) of the two-time correlation plot. Figure 1 shows representative two-time correlation plots from XPCS scans at various states during the curing reaction.

The curing transition is qualitatively described by the features in the two-time correlation plots. Figure 1(a) shows the dynamics early in the curing schedule at $T = 85.9\,°C$. The decorrelation in the intensity (evidenced as a "falloff" of intensity on both sides of a diagonal of two-time correlation plot) suggests that the dynamics are resolved on the observable time scale. The behavior is nearly "at-equilibrium" in the precured state, indicated by the iso-contour lines of the two-time correlation being approximately parallel to the t_{age} diagonal. The feature suggests that the characteristic time scale of the dynamics is not changing significantly with t_{age} over the observed time scale (up to 120 s). The qualitative features in the two-time correlation plot are similar during the temperature ramp to T_{cure}. In Fig. 1(b), the intensity decorrelates symmetrically over the observed time scales. However, the dynamics are considerably faster compared to the precure state, as t_1 and t_2 extend to just 10 s. Finally, once T_{cure} is reached, the two-time correlation plot feature changes drastically. In Fig. 1(c), the intensity decorrelation diverges with increasing t_{age}. Here the behavior is highly non-equilibrium and the importance of the two-time correlation function is highlighted. The decorrelation progresses across the wide time scale window, suggesting that the characteristic time of the dynamics slows down after the temperature reaches T_{cure}.

To access quantitative information about the dynamics, "aged" one-time correlation functions were extracted from the two-time correlation plots. Therefore, at each t_{age} of interest, we calculated a g_2 by averaging $C(q,t_1,t_2)$ around $t_{age} \pm \Delta t_{age}$. The corresponding one-time correlation function becomes a function of q, t_{age}, and delay time $\tau = |t_2 - t_1|$.[35,39,41] The one-time correlation function then follows a typical Kohlrausch–William–Watts (KWW)

stretched/compressed exponential decay expressed by Eq. (3),

$$g_2(q, t_{age}, \tau) = c + \beta(\exp(-2(\Gamma\tau)^\gamma)), \qquad (3)$$

where the characteristic time scale of the dynamics is defined by the relaxation rate Γ (in units of s^{-1}). The exponential decay is further fit by the stretching/compression exponent γ. β is the optical contrast, or Siegert factor, determined by the scattering setup and c is the baseline, which is expected to be 1 for ergodic samples. The values for β were 0.19–0.22, comparable to those found for a static porous glass sample (CoralPor®, SCHOTT), indicating that the cured epoxy did not exhibit any dominant dynamic modes outside of our time window (Fig. S3 of the supplementary material).[36] Curiously, β exhibits a subtle t_{age} dependence where β is lower at $T = 85\,°C$ compared to standard values of the contrast at T_{cure}. It is possible that the lower contrast is due to fast dynamics of the individual particles in the uncured resin, accentuated in the absence of the permanent thermoset network. Similar variability in β has been reported in both colloidal and chemical gelation studies.[31,42,43] However, we cannot resolve such dynamics quantitatively as they exist outside the accessible XPCS time window and q regime in the scattering setup.

We plot a series of evolving correlation functions selected at various t_{age} at a representative q value of $q = 0.0969\,nm^{-1}$ in Fig. 2. Here, g_2 is normalized as $(g_2 - c)/\beta$ so that the exponential decay progresses from an initial value of 1 to a final baseline value of 0. In Fig. 2(a), at $T = 85\,°C$, the decay of g_2 is observable and does not change much with t_{age}. Therefore, in the precured state, the dynamics are indeed at equilibrium, as indicated previously in a qualitative form from the two-time correlation plots. Once the temperature begins to increase from $T = 85\,°C$ to $T = 120\,°C$, the characteristic relaxation rate (Γ) of g_2 rapidly speeds up as the decay shifts to shorter time scales, indicating much faster dynamics. The dynamics speed up by an order of magnitude during the temperature ramp as suggested by the g_2 functions calculated at $T \approx 111\,°C$ [Fig. 2(a)]. Figure 2(b) shows the g_2 functions collected from a

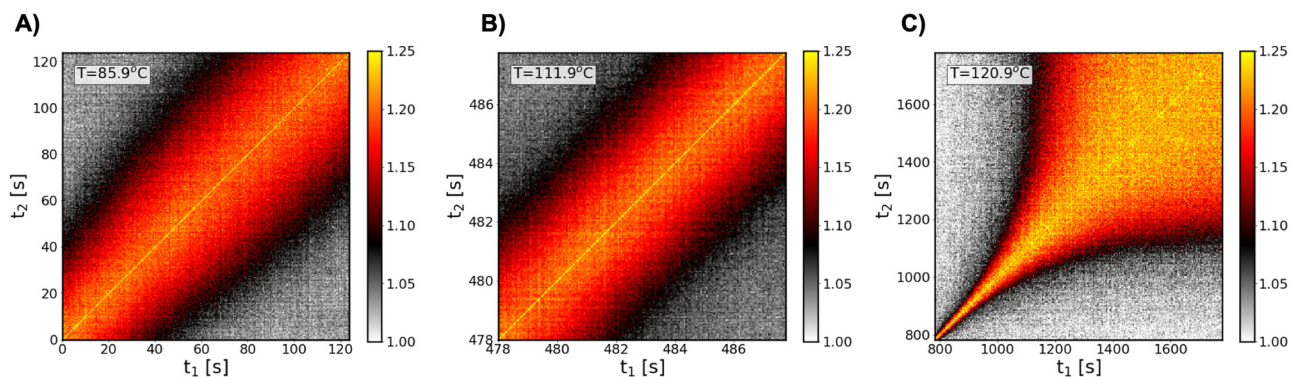**FIG. 1.** Two-time correlation plots of evolving dynamics at various times during curing schedule ($q = 0.0969\,nm^{-1}$). (a) $T = 85.9\,°C$ through isothermal precure; (b) during temperature ramp to T_{cure}; (c) $T = 120.9\,°C$ during isothermal curing. Approximate sample temperature (T) is labeled.
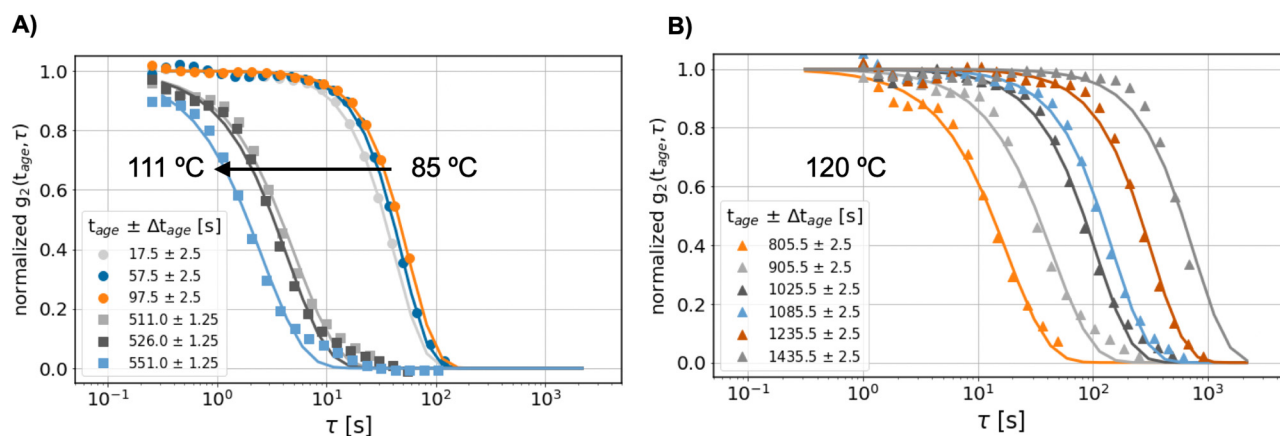
FIG. 2. One-time correlation functions g_2 at various t_{age} along the curing procedure ($q = 0.0969\ nm^{-1}$). g_2 functions are calculated from the two-time correlation plots (symbols) and fit to the stretched/compressed exponential function presented in Eq. (3) (lines). g_2 is normalized according to $(g_2(q, t_{age}, \tau) - c)/\beta$. Typical correlation functions are plotted for the dynamics (a) before T_{cure} is achieved and (b) after T_{cure} is reached and the reaction progresses. During the precure stage and heating ramp, the dynamics are at relative equilibrium. After T_{cure} is reached ($t_{age} > 600\ s$), the dynamics become highly out-of-equilibrium and the characteristic relaxation rate decreases by several orders of magnitude.

series of different t_{age} once the temperature reaches $T_{cure} = 120\ ^\circ C$. The dynamics quickly evolve during the scan as we observed in Fig. 1(c). Γ now shifts over several orders of magnitude to much slower rates. The compression exponent (γ) is consistently greater than 1 across all times and temperatures, suggesting that the dynamic are faster than exponential. At $q = 0.0969\ nm^{-1}$, $\gamma \sim 1.5$ in the precure state at $T = 85\ ^\circ C$ (Fig. S4 of the supplementary material). As T increases to T_{cure}, γ begins to fluctuate toward $\gamma = 1$, initiated by the increase in thermal energy, which is highly out-of-equilibrium but detectable by XPCS. After T_{cure} is reached, γ steadily increases during the remaining cure, approaching $\gamma = 2$. As chemical cross-linking progresses, the filler particles become constrained and as a result, the dynamics appear to become accelerated much faster than simple exponential. At late aging times after reaching a total $t_{age} \approx 1400\ s$ at $T_{cure} = 120\ ^\circ C$, the characteristic time scale of the dynamics (inverse of Γ) slows down to the total exposure time of the XPCS scan, and the decorrelation of g_2 can no longer be determined from the XPCS datasets.

The relaxations are ergodic up to $t_{age} \approx 1400\ s$, however during the cure, a slow decay at long delay times τ was observed and not captured by the KWW expression. As a result, the baseline of the fit deviates slightly from the experimental g_2 in Fig. 2. The slower dynamics could describe the emergence of an additional relaxation mechanism present in late stage curing but are not sensitive enough in XPCS to explore quantitatively.

The q-dependence of Γ is displayed in Fig. 3. We find that Γ scales linearly with q (i.e., $\Gamma \propto q$). The q-dependent dynamics are of particular interest as they describe the type of motion on the microscopic scale, whether it be diffusive or collective.[39] For Brownian motion, $\Gamma \propto q^2$ and the proportionality is the Stokes–Einstein diffusion constant D_0 (where $\Gamma = D_0 q^2$). Linear scaling is observed in various soft matter systems such as colloidal gels, concentrated emulsions, and polymer grafted nanoparticles embedded in polymer matrices.[38,41,44–46] The proposed linear scaling coupled

with compressed exponential of $\gamma = 1.5$ represents collective, ballistic dynamics resulting from strain release from stress dipoles generated in the internal structure.[45] We find that the fillers in the epoxy resin follow similar collective dynamics across all temperatures and
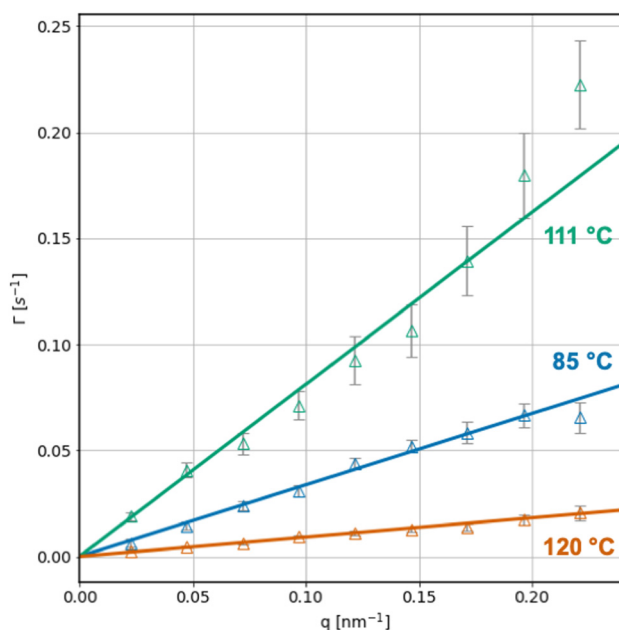

FIG. 3. Relaxation rate (Γ) scales with q and corresponding fits to a linear, ballistic motion model where $\Gamma = V_p q$, where V_p is the local particle velocity. Typical scaling relationships shown for early curing times where temperature is $T = 85\ ^\circ C$, intermediate curing times during the temperature ramp, and later times where T_{cure} is achieved.

04 April 2024 17:16:59

time scales evaluated during the experiment. The q-dependent Γ is plotted at three representative t_{age} during the cure process. The lines in Fig. 3 show the best fits to the experimental data where $\Gamma = V_p q$. V_p is a proportionality constant similar to D_0 but instead represents the ballistic motion of the scatters as a local velocity in units of nm/s.[37,38,45] The precure state at $T = 85\,°C$ (blue symbols) shows a clear linear fit. During the temperature ramp (green symbols) the dynamics speed up as shown by the increase in the slope of the linear fit, which is an increase in the local velocity of the particles. Finally, once T_{cure} is reached and the cross-linking initiates (orange symbols) the slope becomes much less steep, suggesting a drastic decrease of the local particle velocity.

To map out the complete evolution of the nanoscale dynamics during the curing protocol, V_p is calculated across a wide range of t_{age} evaluated during the experiment. We plot the evolution of V_p with time in Fig. 4 along with the temperature of the sample overlaid on the secondary y axis. In the precure state at $T = 85\,°C$, the dynamics are relatively constant where $V_p \approx 0.1$ nm/s. The dynamics quickly speed up by two orders of magnitude as the temperature is ramped up to the $T_{cure} = 120\,°C$. The rapid increase of V_p seems unexpected based on our understanding of the cross-linking of the polymer, which is supposed to slow down the dynamics. However, since a thermo-latent initiator was used in this particular formulation, crosslinking is initiated at around $T \approx 100\,°C$ during the ramping process. The rapid increase in temperature produces more thermal motion in the system, reducing the viscosity of the epoxy resin, thus the particles appear much faster within the precured structural state.

Once T_{cure} is reached and the reaction progresses, the dynamics become slower and quickly decay several orders of magnitude to $V_p \approx 10^{-2}$ nm/s. The final observed dynamics are much slower than in the precure state, especially considering the impact of thermal motion on the particle velocity observed during the heating stage (where the temperature is much higher than in the uncured state).
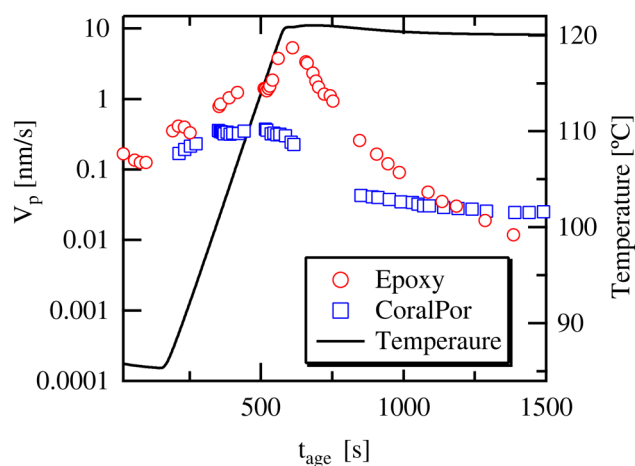

FIG. 4. Evolution of nanoscale dynamics expressed by the local particle velocity ($V_p = \Gamma/q$) over the full curing procedure. Temperature is plotted on the secondary y axis.

Here, the observed dynamics are likely due to a competition between thermally induced motion and restriction from the cross-linking of the polymer network, where the restrictions of the network dominate.

We find that after the curing, the dynamics are equivalent to those measured for the static reference sample of porous glass over an equivalent temperature profile (shown by blue symbols in Fig. 4). The porous glass was glued (Torr Seal®, Varian) to a sample holder of same thermal mass as the sample holder used for the epoxy curing experiment. While this sample is known to be static over the probed time scales at room temperature, the decorrelations observed in the correlation functions are predominantly due to the transient thermal drift (thermal expansion) of the heated sample holder following the temperature ramp.[36] The decorrelations at $t_{age} \geq 1200$ s likely contain contributions from the weakening of the glue at $T_{cure} = 120\,°C$ (which is identical to the maximum use temperature specified for the Torr Seal glue). Therefore, the time scales measured for the epoxy sample for $t_{age} \geq 1200$ s might be reasonable; however, we conservatively restrict our quantitative analysis to the ages where the relaxation rates from the epoxy system are higher than the relaxation rates of the reference sample. In any case, we can qualitatively identify that the epoxy undergoes solidification after $t_{age} = 1200$ s at $T_{cure} = 120\,°C$ according to two-time correlation functions well beyond the recommended curing time (Fig. S5 of the supplementary material).

In addition to the dynamics, the microstructure of the epoxy is also resolved through the time-resolved radial averaging of the small angle x-ray scatting (SAXS) intensity $I(q)$. The data are plotted in the supplementary material (Fig. S6) as $I(q)$ at representative t_{age} from XPCS datasets taken in the uncured ($T = 85\,°C$) and post-cure ($T = 120\,°C$) states. Power-law q-dependence [i.e., $I(q) \propto q^{-P}$] is observed at both stages. The particle sizes of alumina trihydrate and boron nitride are larger than the length scales resolved within the q range, so the structure factor [$S(q)$] is not picked up on the detector. The power law ($p \approx 3.5$–3.6) is close to the typical Porod scaling ($p = 4$), which corresponds to the scattering from a smooth interface.[47,48] While the background scattering was not subtracted, a deviation from such scaling may be reasonable considering the filler surface morphology from SEM (i.e., surface fractal). Future experiments are warranted for clarification. The size dispersity is unlikely to contribute to the $I(q)$ scaling in this q regime.[49] Large dispersity is known to affect the dynamics in dilute suspensions of non-interacting particles, where the temporal correlation function can be expressed as a sum of exponential functions.[50,51] However, the concentration of the alumina filler is 25 wt. %, such that the above approximation is invalid. Analysis of XPCS correlation functions in the highly loaded regime is currently lacking and require additional investigation. We do not see any significant changes in the SAXS profiles over time for the uncured and cured samples. In addition, the scattering profiles remained nearly unchanged before and after the curing process, indicating that the contributions from the network structure (if any) are too small to see for the present case. The contribution of the thermosetting polymer network (whose mesh size/correlation length is likely within the observed q range) to the scattering signal is not conclusive. Spatially heterogeneous structure development is of considerable interest and will be investigated in more detail by

independent SAXS measurements with further corrections for air scattering and absorption or small angle neutron scattering (SANS) measurements which could provide a stronger contrast mechanism for the polymer matrix.

The XPCS measurements were compared to a more traditional macroscale characterization of the epoxy curing reaction (DSC). The epoxy was prepared and heated through a curing schedule identical to the one used in XPCS experiments. In Fig. 5, we plot the normalized heat flow (exothermic up) as a function of time with the sample temperature overlaid in a similar fashion to the XPCS results shown in Fig. 4. Both curves for the sample during curing and post curing have been rescaled according to the sample mass (W/g) and the baseline was shifted for clarity.

At $T = 85\,°C$ equilibration, the heat flow is stable and does not change for either scan (during curing or fully cured). Upon heating through temperature ramp, the heat flow begins to increase (exothermic) as the sample absorbs some of the heat. At approximately $T = 100\,°C$, a significant exothermic event is observed in comparison to the fully cured sample and the heat flow begins to increase dramatically. Once the temperature reaches T_{cure}, the heat flow begins to decrease and decay back to the static baseline value of the cured sample. The difference in integrated area between the curing and cured scans from $t_{age} = 200\,s$ to $t_{age} = 1600\,s$ is ~100 Ws/g, due to exothermic heat given off during the cross-linking reaction. The deviation at $T = 105\,°C$ ($t_{age} \approx 450\,s$) indicates that the cross-linking indeed initiates before T_{cure} is reached. The comparison of the DSC and XPCS shows that the reaction is clearly finished after about 400 s (corresponding to $t_{age} = 1000\,s$ in the measurement). However, the dynamics resolved by XPCS continue to decay for at least 600 s after T_{cure} is reached, as the polymer chains become glassy at the microscopic scale. At the same time, the XPCS results suggest that the cure process involves at least two different kinetics: the very fast curing kinetics at $t_{age} < 800\,s$ and subsequent slowing
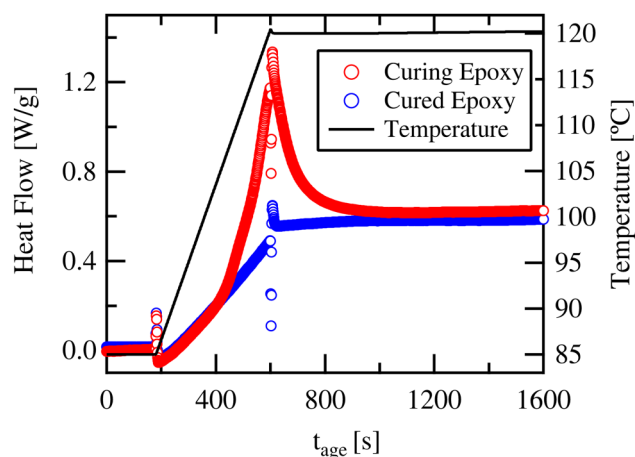

FIG. 5. Differential scanning calorimetry (DSC) heat flow traces collected during curing of epoxy adhesive (blue curve) and immediately after curing (red curve) as a function of time during the curing protocol. Corresponding temperature (black line) plotted on the secondary y axis.

down before the solidification. While it is known that certain epoxy curing schemes involve multiple steps with different activation energies, the different reactions speeds are likely related to the buildup of T_g with time.[52] The reaction rate will be highest when T_{cure} is higher than the T_g at a given time. Additionally, the local increase in viscosity due to the progression of the cure results in slower diffusion of monomers and reduced reactivity of the alcohol groups due to lower mobility of the polymer chains. Further XPCS and DSC experiments are currently in progress to fully develop the out-of-equilibrium dynamics–property relationships observed in the epoxy curing process.

The curing of the epoxy falls into the discussion of well-known solidification transitions such as glass transition and gelation, which also exhibit dynamics described by KWW-type exponential processes. For example, the dynamics in the vicinity of the glass transition of colloidal glass formers is universally described by stretched exponentials ($\gamma < 1$).[53–55] As the volume fraction (ϕ) of spherical particles with hard-sphere potential increases to the critical limit of $\phi_g = 0.58$, Γ decreases and the terminal decay of the correlation function becomes stretched.[53] The stretched exponential behavior arises from the slow motion of the particle as it escapes the constrained "cage" formed by its neighbors (known as the α relaxation).[45] Although the dynamics do slowdown in the epoxy upon formation of a network structure and onset of T_g, the characteristics of the nanoscale dynamics revealed by XPCS ($\Gamma \propto q^1$ and $\gamma > 1$) indicate that the curing is not attributed to the glass transition but gelation. Evolution of the dynamics through gelation (chemical and physical) has been extensively studied in rheology, DLS, and even XPCS for polymeric, colloidal, and thermo-reversible gel systems.[30–32,56–59] Much is known about the liquid–solid transition in commercial epoxies as well.[14,15,18,60] The epoxy curing characterized here does not follow a traditional sol-gel transition through exclusively physical or chemical gelation. In the precured state, significant physical interactions are present between the filler and prepolymer resin for viscosity modification, which gives the resin a "paste" like response. The hyper-diffusive dynamics suggest that the physical interactions are restricting the filler motion in the prepolymer. Once the curing is initiated, we understand that the polymerization is chemical in nature, yet hyper-diffusive dynamics are still universally observed. The rapid fluctuations of γ during the cure suggest a transition between independent structural mechanisms. Our results conclude that the epoxy curing portrays signatures of traditional gelation and the competition of physical interactions and chemical gelation are convoluted into the dynamics of the filler particles. The steady increase in γ once T_{cure} is reached is intriguing and deviates from the theoretical values of $\Gamma \propto q^1$ and $\gamma = 1.5$, predicted from the strain release of randomly distributed stress dipoles generated in the internal structure.[44,45] A limit of $\gamma = 2$ with $\Gamma \propto q^1$ was previously observed during stress relaxation of chemically bonded resorcinol-formaldehyde (RF) aerogels.[39] It was proposed that the length scale of the stress points were correlated into regions on the order of the molecular size (~1 nm) as opposed to the randomly distributed stress dipoles. A similar stress relaxation mechanism is possible as the late-stage solidification of the epoxy could introduce trapped static structures as T_g increases, resulting in correlated relaxation zones on the order of the thermoset mesh size. However, due to the uncertainty of the dynamics in this

regime (with respect to the porous glass sample) and the potential impact of particle size dispersity on dynamics in highly filled nanocomposites, a quantitative comparison with the theory is difficult. Nevertheless, our conclusion is evident that the curing kinetics are hyper-diffusive at the microscopic scale regardless of the curing stages, which is a new finding with XPCS.

The physics of gelation and cross-linking are complex, especially during a thermally activated, out-of-equilibrium curing procedure. The true determination of a gel point as well as a gel time are of upmost importance. In an ideal case, the thermosetting network formation is modeled by a fractal network. The gel point and gel time are then dependent on the molecular design of the epoxy (notably the stoichiometric ratio and functionality).[15] A correlation of the observed dynamics by XPCS to the theoretical network formation is desired but requires additional simulation and modeling of the system. It is worth deconvoluting the competition between physical interactions and chemical gelation in the industrial formulations of interest. For such work, a model material system with well-defined filler particle size and narrow dispersity may be necessary.

CONCLUSIONS

We demonstrate that x-ray photon correlation spectroscopy (XPCS) is an appropriate technique to track the progression of a typical curing reaction for a thermally triggered industrial epoxy adhesive. The local dynamics of filler particles probe the formation of a thermoset from the uncured state through the curing at elevated temperature T_{cure}. The dynamics of inorganic filler particles are used to probe the formation of the thermoset network. The dynamics decay rapidly during the curing and are compared to the exothermic heat flow observed in DSC. XPCS provides a new microscopic viewpoint to quantitatively describe the curing process.

It is necessary for such industrial materials and applications to provide deeper insight into the mechanisms that determine the material performance. Most in-lab characterizations are either qualitative or only evaluate exclusively macroscale behaviors and responses. With XPCS, the nanoscale dynamics are directly measured and can be correlated to the macroscale response to develop stronger dynamics–property relationships. The potential to investigate the cross-linking after gelation is appealing as rheology is limited due to excessive shear forces. There are potential benefits for understanding time-dependent material properties at the later stages of the cross-linking reaction, e.g., calculating the development of the residual stresses in the adhesive bond line or the development of bond strength during the continuous oven cure process. Therefore, as an established technique, XPCS should be used to investigate different curing processes or temperature profiles for such industrial epoxy materials.

SUPPLEMENTARY MATERIAL

See the supplementary material for the SEM results of the fillers, additional details of the XPCS analysis, and the SAXS results for the epoxy samples before and after the curing process.

REFERENCES

[1]F. L. Jin, X. Li, and S. J. Park, "Synthesis and application of epoxy resins: A review," J. Ind. Eng. Chem. **29**, 1–11 (2015).

[2]S. Sprenger, "Epoxy resin composites with surface-modified silicon dioxide nanoparticles: A review," J. Appl. Polym. Sci. **130**(3), 1421–1428 (2013).

[3]A. A. Azeez, K. Y. Rhee, S. J. Park, and D. Hui, "Epoxy clay nanocomposites—Processing, properties and applications: A review," Compos. Part B Eng. **45**(1), 308–320 (2013).

[4]C. P. R. Nair, "Advances in addition-cure phenolic resins," Prog. Polym. Sci. **29**(5), 401–498 (2004).

[5]H. Q. Pham and M. J. Marks, "Epoxy resins," in *Ullmann's Encyclopedia of Industrial Chemistry* (Wiley VCH, 2005).

[6]L. Shechter and J. Wynstra, "Glycidyl ether reactions with alcohols, phenols, carboxylic acids, and acid anhydrides," Ind. Eng. Chem. **48**(1), 86–93 (1956).

[7]M. I. Childers, J. M. Longo, N. J. Van Zee, A. M. Lapointe, and G. W. Coates, "Stereoselective epoxide polymerization and copolymerization," Chem. Rev. **114**(16), 8129–8152 (2014).

[8]C. H. Behrens and K. B. Sharpless, "Selective transformations of 2,3-epoxy alcohols and related derivatives. Strategies for nucleophilic attack at carbon-3 or carbon-2," J. Org. Chem. **50**(26), 5696–5704 (1985).

[9]V. Trappe, W. Burchard, and B. Steinmann, "Anhydride-cured epoxies via chain reaction. 1. The phenyl glycidyl ether/phthalic acid anhydride system," Macromolecules **24**(17), 4738–4744 (1991).

[10]A. O. Konuray, X. Fernández-Francos, and X. Ramis, "Analysis of the reaction mechanism of the thiol-epoxy addition initiated by nucleophilic tertiary amines," Polym. Chem. **8**(38), 5934–5947 (2017).

[11]F. Wu, X. Zhou, and X. Yu, "Reaction mechanism, cure behavior and properties of a multifunctional epoxy resin, TGDDM, with latent curing agent dicyandiamide," RSC Adv. **8**(15), 8248–8258 (2018).

[12]I. A. Saeedi, T. Andritsch, and A. S. Vaughan, "On the dielectric behavior of amine and anhydride cured epoxy resins modified using multi-terminal epoxy functional network modifier," Polym. Basel **11**(8), 1271 (2019).

[13]J. P. Pascault and R. J. J. Williams, "Glass transition temperature versus conversion relationships for thermosetting polymers," J. Polym. Sci. Part B Polym. Phys. **28**(1), 85–95 (1990).

[14]H. Yu, S. G. Mhaisalkar, and E. H. Wong, "Observations of gelation and vitrification of a thermosetting resin during the evolution of polymerization shrinkage," Macromol. Rapid Commun. **26**(18), 1483–1487 (2005).

[15]L. Granado, S. Kempa, L. J. Gregoriades, F. Brüning, A.-C. Genix, J.-L. Bantignies, N. Fréty, and E. Anglaret, "*In situ* vibrational probes of epoxy gelation," ACS Macro Lett. **8**(8), 984–988 (2019).

[16]R. Hardis, J. L. P. Jessop, F. E. Peters, and M. R. Kessler, "Cure kinetics characterization and monitoring of an epoxy resin using DSC, Raman spectroscopy, and DEA," Compos. Part A **49**, 100–108 (2013).

[17]H. H. Winter and M. Mours, "Rheology of polymers near liquid-solid transitions," Adv. Polym. Sci. **134**, 165–234 (1997).

[18]J. P. Eloundou, M. Feve, J. F. Gerard, D. Harran, and J. P. Pascault, "Temperature dependence of the behavior of an epoxy-amine system near the

gel point through viscoelastic study. 1. Low-T_g epoxy-amine system," Macromolecules **29**(21), 6907–6916 (1996).

[19]P. Musto, M. Abbate, G. Ragosta, and G. Scarinzi, "A study by Raman, near-infrared and dynamic-mechanical spectroscopies on the curing behaviour, molecular structure and viscoelastic properties of epoxy/anhydride networks," Polym. Guildf **48**(13), 3703–3716 (2007).

[20]M. Aldridge, A. Wineman, A. Waas, and J. Kieffer, "*In situ* analysis of the relationship between cure kinetics and the mechanical modulus of an epoxy resin," Macromolecules **47**(23), 8368–8376 (2014).

[21]J. Mijović and S. Andjelić, "A study of reaction kinetics by near-infrared spectroscopy. 1. Comprehensive analysis of a model epoxy/amine system," Macromolecules **28**(8), 2787–2796 (1995).

[22]J. Mijović, S. Andjelić, and J. M. Kenny, "*In situ* real-time monitoring of epoxy/amine kinetics by remote near infrared spectroscopy," Polym. Adv. Technol. **7**(1), 1–16 (1996).

[23]A. Nogales and A. Fluerasu, "X ray photon correlation spectroscopy for the study of polymer dynamics," Eur. Polym. J. **81**, 494–504 (2016).

[24]R. L. Leheny, "XPCS: Nanoscale motion and rheology," Curr. Opin. Colloid Interface Sci. **17**(1), 3–12 (2012).

[25]S. K. Kumar, B. C. Benicewicz, R. A. Vaia, and K. I. Winey, "50th anniversary perspective: Are polymer nanocomposites practical for applications?," Macromolecules **50**, 714–731 (2017).

[26]O. G. Shpyrko, "X-ray photon correlation spectroscopy," J. Synchr. Radiat. **21**(5), 1057–1064 (2014).

[27]K. Nygård, J. Buitenhuis, M. Kagias, K. Jefimovs, F. Zontone, and Y. Chushkin, "Anisotropic de Gennes narrowing in confined fluids," Phys. Rev. Lett. **116**(16), 1–5 (2016).

[28]Q. Zhang, E. M. Dufresne, S. Narayanan, P. Maj, A. Koziol, R. Szczygiel, P. Grybos, M. Sutton, and A. R. Sandy, "Sub-microsecond-resolved multi-speckle x-ray photon correlation spectroscopy with a pixel array detector," J. Synchr. Radiat. **25**(5), 1408–1416 (2018).

[29]Y. Shinohara, H. Kishimoto, T. Maejima, H. Nishikawa, N. Yagi, and Y. Amemiya, "X-ray photon correlation spectroscopy of filler in rubber," Jpn. J. Appl. Phys. Part 2 **46**(12–16), L300–L302 (2007).

[30]Y. Shinohara, H. Kishimoto, T. Maejima, H. Nishikawa, M. Takata, and Y. Amemiya, "Observation of filler dynamics in rubber with X-ray photon correlation spectroscopy," IOP Conf. Ser. Mater. Sci. Eng. **24**, 012005 (2011).

[31]O. Czakkel and A. Madsen, "Evolution of dynamics and structure during formation of a cross-linked polymer gel," Eur. Phys. Lett. **95**(2), 28001 (2011).

[32]B. Ruta, O. Czakkel, Y. Chushkin, F. Pignon, R. Nervo, F. Zontone, and M. Rinaudo, "Silica nanoparticles as tracers of the gelation dynamics of a natural biopolymer physical gel," Soft Matter **10**(25), 4547–4554 (2014).

[33]T. Matsunaga and M. Shibayama, "Gel point determination of gelatin hydrogels by dynamic light scattering and rheological measurements," Phys. Rev. E Stat. Nonlinear Soft Matter Phys. **76**(3), 303001(R) (2007).

[34]T. Koga, C. Li, M. K. Endoh, J. Koo, M. Rafailovich, S. Narayanan, D. R. Lee, L. B. Lurio, and S. K. Sinha, "Reduced viscosity of the free surface in entangled polymer melt films," Phys. Rev. Lett. **104**(6), 10–13 (2010).

[35]K. J. Johnson, L. Wiegart, A. C. Abbott, E. B. Johnson, W. Baur, and H. Koerner, "In operando monitoring of dynamic recovery in 3D-printed thermoset nanocomposites by XPCS," Langmuir **35**(26), 8758–8768 (2019).

[36]S. K. Abeykoon, Y. Zhang, E. D. Dill, T. A. Caswell, D. B. Allan, A. Akilic, L. Wiegart, S. Wilkins, A. Heroux, K. K. Van Dam *et al.*, "Software tools for x-ray photon correlation and x-ray speckle visibility spectroscopy," in *2016 New York Scientific Data Summit (NYSDS)* (IEEE, 2016).

[37]H. Guo, G. Bourret, M. K. Corbierre, S. Rucareanu, R. B. Lennox, K. Laaziri, L. Piche, M. Sutton, J. L. Harden, and R. L. Leheny, "Nanoparticle motion within glassy polymer melts," Phys. Rev. Lett. **102**(7), 20–23 (2009).

[38]R. Mangal, S. Srivastava, S. Narayanan, and L. A. Archer, "Size-dependent particle dynamics in entangled polymer nanocomposites," Langmuir **32**(2), 596–603 (2016).

[39]A. Madsen, R. L. Leheny, H. Guo, M. Sprung, and O. Czakkel, "Beyond simple exponential correlation functions and equilibrium dynamics in X-ray photon correlation spectroscopy," New J. Phys. **12**, 055001 (2010).

[40]A. Malik, A. R. Sandy, L. B. Lurio, G. B. Stephenson, S. G. J. Mochrie, I. Mc Nulty, and M. Sutton, "Coherent x-ray study of fluctuations during domain coarsening," Phys. Rev. Lett. **81**(26), 5832–5835 (1998).

[41]A. Fluerasu, A. Moussaïd, A. Madsen, and A. Schofield, "Slow dynamics and aging in colloidal gels studied by x-ray photon correlation spectroscopy," Phys. Rev. E Stat. Nonlinear Soft Matter Phys. **76**(1), 3–6 (2007).

[42]J. L. Harden, H. Guo, M. Bertrand, T. N. Shendruk, S. Ramakrishnan, and R. L. Leheny, "Enhanced gel formation in binary mixtures of nanocolloids with short-range attraction," J. Chem. Phys. **148**(4), 044902 (2018).

[43]H. Guo, S. Ramakrishnan, J. L. Harden, and R. L. Leheny, "Gel formation and aging in weakly attractive nanocolloid suspensions at intermediate concentrations," J. Chem. Phys. **135**(15), 154903 (2011).

[44]L. Cipelletti, S. Manley, R. C. Ball, and D. A. Weitz, "Universal aging features in the restructuring of fractal colloidal gels," Phys. Rev. Lett. **84**(10), 2275–2278 (2000).

[45]L. Cipelletti, L. Ramos, S. Manley, E. Pitard, D. A. Weitz, E. E. Pashkovski, and M. Johansson, "Universal non-diffusive slow dynamics in aging soft matter," Faraday Discuss. **123**(1), 237–251 (2003).

[46]R. Bandyopadhyay, D. Liang, H. Yardimci, D. A. Sessoms, M. A. Borthwick, S. G. J. Mochrie, J. L. Harden, and R. L. Leheny, "Evolution of particle-scale dynamics in an aging clay suspension," Phys. Rev. Lett. **93**(22), 2–5 (2004).

[47]A.-C. Genix and J. Oberdisse, "Structure and dynamics of polymer nanocomposites studied by X-ray and neutron scattering techniques," Curr. Opin. Colloid Interface Sci. **20**(4), 293–303 (2015).

[48]A.-C. Genix and J. Oberdisse, "Nanoparticle self-assembly: From interactions in suspension to polymer nanocomposites," Soft Matter **14**, 5161–5179 (2018).

[49]W. H. De Jeu, *Basic X-Ray Scattering for Soft Matter*, 1st ed. (Oxford University Press, Oxford, 2016).

[50]S. R. Aragón and R. Pecora, "Theory of dynamic light scattering from polydisperse systems," J. Chem. Phys. **64**(6), 2395–2404 (1976).

[51]P. N. Pusey, H. M. Fijnaut, and A. Vrij, "Mode amplitudes in dynamic light scattering by concentrated liquid suspensions of polydisperse hard spheres," J. Chem. Phys. **77**(9), 4270–4281 (1982).

[52]N. Sbirrazzuoli and S. Vyazovkin, "Learning about epoxy cure mechanisms from isoconversional analysis of DSC data," Thermochim. Acta **388**(1–2), 289–298 (2002).

[53]W. Van Megen and P. N. Pusey, "Dynamic light-scattering study of the glass transition in a colloidal suspension," Phys. Rev. A **43**(10), 5429–5441 (1991).

[54]D. Lumma, L. B. Lurio, M. A. Borthwick, P. Falus, and S. G. J. Mochrie, "Structure and dynamics of concentrated dispersions of polystyrene latex spheres in glycerol: Static and dynamic x-ray scattering," Phys. Rev. E **62**(6), 8258–8269 (2000).

[55]P. Wochner, C. Gutt, T. Auternrieth, T. Demmer, V. Bugaev, A. Diaz Ortiz, A. Duri, F. Zontone, G. Grubel, and H. Dosch, "X-ray cross correlation analysis uncovers hidden local symmetries in disordered matter," Proc. Natl. Acad. Sci. U.S.A. **106**(28), 11511–11514 (2009).

[56]H. H. Winter, "Glass transition as the rheological inverse of gelation," Macromolecules **46**(6), 2425–2432 (2013).

[57]L. Frenzel, F. Lehmkühler, I. Lokteva, S. Narayanan, M. Sprung, and G. Grübel, "Anomalous dynamics of concentrated silica-PNIPAm nanogels," J. Phys. Chem. Lett. **10**(17), 5231–5236 (2019).

[58]L. Frenzel, F. Lehmkühler, M. Koof, I. Lokteva, and G. Grübel, "The phase diagram of colloidal silica-PNIPAm core-shell nanogels," Soft Matter **16**(2), 466–475 (2020).

[59]Q. Zhang, D. Bahadur, E. M. Dufresne, P. Grybos, P. Kmon, R. L. Leheny, P. Maj, S. Narayanan, R. Szczygiel, S. Ramakrishnan *et al.*, "Dynamic scaling of colloidal gel formation at intermediate concentrations," Phys. Rev. Lett. **119**(17), 1–6 (2017).

[60]D. Lairez, J. R. Emery, D. Durand, and M. Adam, "Rheological behavior of an epoxy/amine system near the gel point," Macromolecules **25**(1), 286–289 (1992).

04 April 2024 17:16:59